



PERGAMON

Available online at www.sciencedirect.com

SCIENCE @ DIRECT®

Vision Research 43 (2003) 2197–2205

Vision
Research

www.elsevier.com/locate/visres

Orientation opponency in human vision revealed by energy-frequency analysis

Isamu Motoyoshi*, Frederick A.A. Kingdom

McGill Vision Research Unit, 687 Pine Avenue West, Rm H4-14, Montreal, Que., Canada H3A 1A1

Received 4 February 2003; received in revised form 5 April 2003

Abstract

Studies of second-order visual processing have primarily been concerned with understanding the mechanisms for detecting *spatiotemporal* variations in such attributes as contrast, orientation, spatial frequency, etc. Here, we have examined the *orientation* characteristics of second-order processes using bandpass noise whose Fourier energy is sinusoidally modulated across orientation, rather than across space or time. Sensitivity for detecting orientation-energy modulations was measured as a function of modulation frequency. The sensitivity function was bandpass, with a pronounced peak at an orientation frequency of 4 cycles/ π . An inverse Fourier transform of the sensitivity function revealed a filter profile displaying a centre-surround antagonism across orientation, with an excitatory centre within 6–9 deg and inhibitory lobes at 15–20 deg from the filter's centre. The degree of centre-surround antagonism increased with stimulus size far beyond the spatial range of the first-order filters (more than 64 times the dominant spatial wavelength of the noise carrier). These results suggest that second-order processing involves 'orientation-opponent' channels that extract differences in first-order outputs across orientation over a wide area of the visual field.

© 2003 Elsevier Ltd. All rights reserved.

Keywords: Second-order; Orientation; Opponency; Texture

1. Introduction

The human visual system is sensitive not only to first-order stimuli, i.e. stimuli varying in luminance or colour, but also to second-order stimuli, which vary in such attributes as contrast, orientation, spatial frequency, binocular disparity and direction-of-motion. The perception of second-order stimuli has been most recently modelled as a two stage process (Chubb & Sperling, 1988; Graham, 1994; Landy & Bergen, 1991; Malik & Perona, 1990; Wilson, 1993), the first stage consisting of a bank of linear filters that are selectively sensitive to luminance- or colour-contrasts at particular orientations, spatial frequencies, disparities and directions-of-motion, and the second stage consisting of larger filters that detect changes in the rectified (or similarly non-linearly transformed) output of the first stage filters.

One of the outstanding issues concerning second-order processes is whether second-order filters pool (rectified)

first-order signals across dimensions other than space and time. The majority of studies of second-order vision have investigated its spatiotemporal properties, by measuring, for example, sensitivity to second-order stimuli that are sinusoidally modulated in the critical attribute across space and/or time (Arsenault, Wilkinson, & Kingdom, 1999; Chubb & Sperling, 1988; Gray & Regan, 1998; Kingdom, Keeble, & Moulden, 1995; Kingdom & Keeble, 1996; Landy & Oruc, 2002; Sutter, Sperling, & Chubb, 1995; Tyler, 1974; Watson & Eckert, 1994), as in the example of the contrast modulated stimulus shown in Fig. 1a. In the main, the results of these studies have been modelled under the assumption that second-order mechanisms spatiotemporally pool the rectified outputs of *just one type* of first-order input (Graham, 1994; Kingdom et al., 1995; Landy & Oruc, 2002; Wilson, 1993). In theory however, second-order mechanisms may receive first-order inputs distributed not only across space and time, but across dimensions such as orientation, spatial frequency, direction of motion, and binocular disparity. Thus second-order mechanisms might embody interactions between different first-order inputs *within* a dimension, for example

* Corresponding author. Tel.: +1-514-842-1231x34756; fax: +1-514-843-1691.

E-mail address: imotoy@po-box.mcgill.ca (I. Motoyoshi).

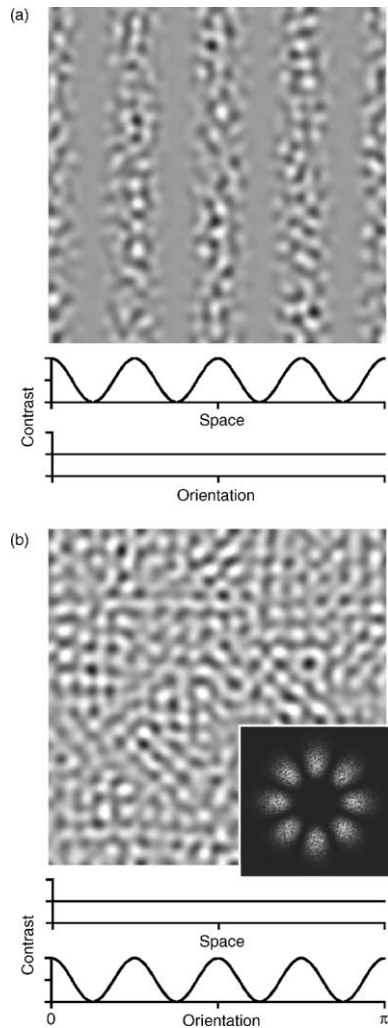


Fig. 1. (a) Contrast modulation across space. The carrier is a band-pass visual noise. (b) Contrast modulation across orientation. Fourier energy of the noise is sinusoidally modulated along orientation. Inset is a Fourier spectrum of the image.

inhibitory and/or excitatory interactions between different orientations, different binocular disparities, etc.

How might one reveal such ‘cross-attribute’ interactions? One method is to measure sensitivity to stimuli that are modulated *not* across space or time, but across the other dimensions of interest. Although several studies have employed this method to study the characteristics of colour and texture processing (Barlow, 1982; Goda & Fujii, 2001; Keeble, Kingdom, Moulden, & Morgan, 1995), none of them has found clear evidence of cross-attribute interactions. In this communication we have examined sensitivity to sinusoidal modulations in the Fourier energy (contrast) of band-pass-filtered noise textures across orientation (Fig. 1b). Our results have revealed a substantial degree of cross-orientation antagonism, which we term orientation opponency.

2. Methods

2.1. Stimuli

Visual stimuli were static, band-pass noise textures whose Fourier energy was radially modulated in a sinusoidal waveform with various orientation frequencies (Fig. 2b–d). The orientation frequency refers the number of cycles of energy modulation from 0 to 180 deg, given as cycle/ π . The centre spatial frequency of the noise was 0.9, 1.7, 3.4, or 6.9 cycles/deg, and the bandwidth 0.75 octaves. The stimuli were presented in a circular window with diameters of 2.3, 4.6, 9.3, or 18.6 deg, on a uniform background of 36 (H) \times 28 (V) deg. The edge of the circular window was vignetted by the positive part of a cosine function with a wavelength of 2.3 deg. The stimuli were generated afresh each trial by means of a fast Fourier transform (FFT) conducted on

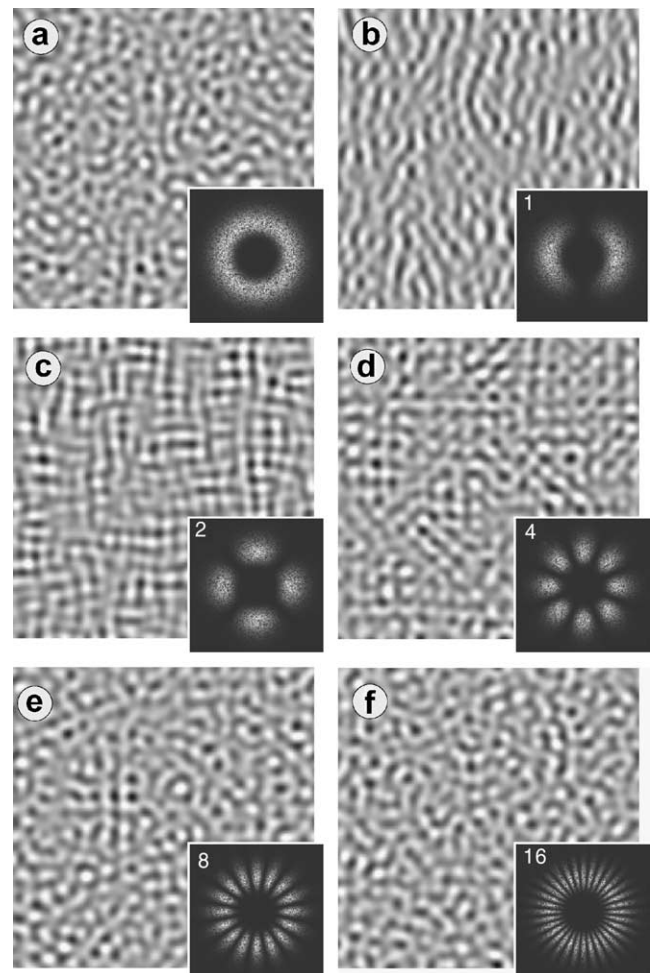


Fig. 2. Stimuli used in the experiment. (a) Isotropic band-pass noise and its Fourier spectrum, showing the absence of modulation along orientation. (b–f) Non-isotropic band-pass noise whose Fourier energy is sinusoidally modulated along orientation with frequencies of 1, 2, 4, 8, 16 cycle/ π .

uniform noise of 512×512 (for the diameter of 18.6 deg) pixels or 256×256 pixels (for the others). The mean luminance of the stimulus was the same as that of the background, at 52 cd/m^2 . The luminance contrast of the stimuli was randomly set on every presentation within a range of 0.75–0.85 Michelson contrast. The ‘phase’ in the orientation domain of energy modulation was also randomly selected for each trial. The various randomisations were designed to minimise the possibility that local luminance cues could be used for detection.

2.2. Procedure

The threshold modulation depth was measured with a two-alternative forced-choice procedure. On each trial, two noise stimuli were presented for 500 ms each, separated by a uniform blank field of 500 ms. One of the stimuli was energy modulated across orientation and the other was not, i.e. was isotropic. Subjects fixated a small point centred on the display and indicated by a button press which stimulus was energy modulated. Auditory feedback was given for an incorrect response. The depth of energy modulation was varied in accordance with a procedure that incorporated three randomly interleaved staircases (one-up-two-down with a step size of 1.0 dB), which was terminated when one of the three staircases reached four reversals. At least six three-staircase measurements were made per condition in separate blocks. Thresholds were calculated from all the binary responses using maximum-likelihood estimation. Sensitivity to orientation-energy modulation was defined as the inverse of the threshold modulation depth.

2.3. Apparatus

All stimuli were generated with a video-graphics board (Cambridge Research Systems VSG2/5) hosted by a PC (Gateway MNT Pro S-P4) and presented on a 21 in. CRT monitor (SONY GDM-F500). The monitor had a frame rate of 120 Hz and a spatial resolution of 1 min/pixel at the viewing distance of 61.5 cm we adopted. Gamma correction was achieved with the use of a 14-bit pixel luminance look-up table.

2.4. Subjects

The two authors (IM and FK) and two naïve observers (LH and SK) served as subjects. All had corrected-to-normal vision.

3. Results

Fig. 3a plots sensitivity as a function of orientation frequency for various sizes of the stimulus field.¹ The carrier spatial frequency of the noise was fixed at 3.4 cycles/deg. The functions have a clear band-pass shape when the stimulus field is relatively large. Sensitivity peaks at around 4 cycles/ π ; paradoxically, it was easier to detect the four-bands-of-orientation, ‘star-shaped’ stimulus in Fig. 2d than the one-band-of-orientation, ‘line-shaped’ stimulus in Fig. 2b.

Using linear system analysis, we estimated the orientation characteristics of the putative second-order filters subserving detection in our task by means of inverse-Fourier transforms of the sensitivity functions in Fig. 3a. The functions were fitted by a sum-of-two-exponentials, given as $S = a \exp(-\alpha |\log_2(f_\theta/F_\theta)|) + b \exp(-\beta f_\theta^2)$, where f_θ is the orientation frequency and the other parameters free parameters. The fits are the lines in Fig. 3a.² Fig. 3b shows the resulting line spread functions estimated for each stimulus size. The profiles reveal a centre-surround antagonism across orientation with an excitatory centre at orientations within 6–9 deg, strong inhibitory lobes centred at 15–20 deg. The profiles also show secondary, weak excitatory lobes centred at 40–60 deg, but one must treat these with caution as they are possibly artifacts of the double exponential used to fit the data.

¹ In our stimuli, the actual amplitude of energy modulation relative to the designated level decreased both as the stimulus size decreased and as the carrier spatial frequency decreased. The decrease was more profound for stimuli with higher orientation frequencies. To take into account this potential artefact, we measured the modulation amplitude for each stimulus condition from the average Fourier energy of 300 sample images. The analysis revealed that the actual modulation amplitude in the smallest stimulus was less than 30% of that of the largest stimulus at an orientation frequency of 20 cycles/ π , and about 80% at 4 cycles/ π . The sensitivity measures were then recast to take into account the physical reduction in amplitude caused by this attenuation. While affecting absolute sensitivity the compensation was found not to significantly affect the overall shapes of the sensitivity functions.

² The sum-of-two-exponentials function was chosen to match as closely as possible the shape of the sensitivity functions. The function did not fit the data for the smallest size (2.3 deg) and lowest spatial frequency (0.9 cycles/deg), but qualitatively similar line-spread functions were obtained when sensitivity functions were interpolated and extrapolated with straight lines. Because of the limited resolution of the stimulus image in the Fourier domain, energy modulations of high orientation frequencies were subject to the effects of aliasing, and hence contained significant amounts of low orientation-frequency energy. The observed sensitivities at high orientation frequencies were thus almost certainly enhanced by these low-frequency components. The artefactual enhancement is however taken into account in the curve fitting to the sensitivity data, in which (a) the predicted filter’s response was estimated by directly convolving the energy modulations in the stimulus by the line spread function given as an inverse FFT of the exponential function, and then (b) the max of the response was compared with the observed sensitivity.

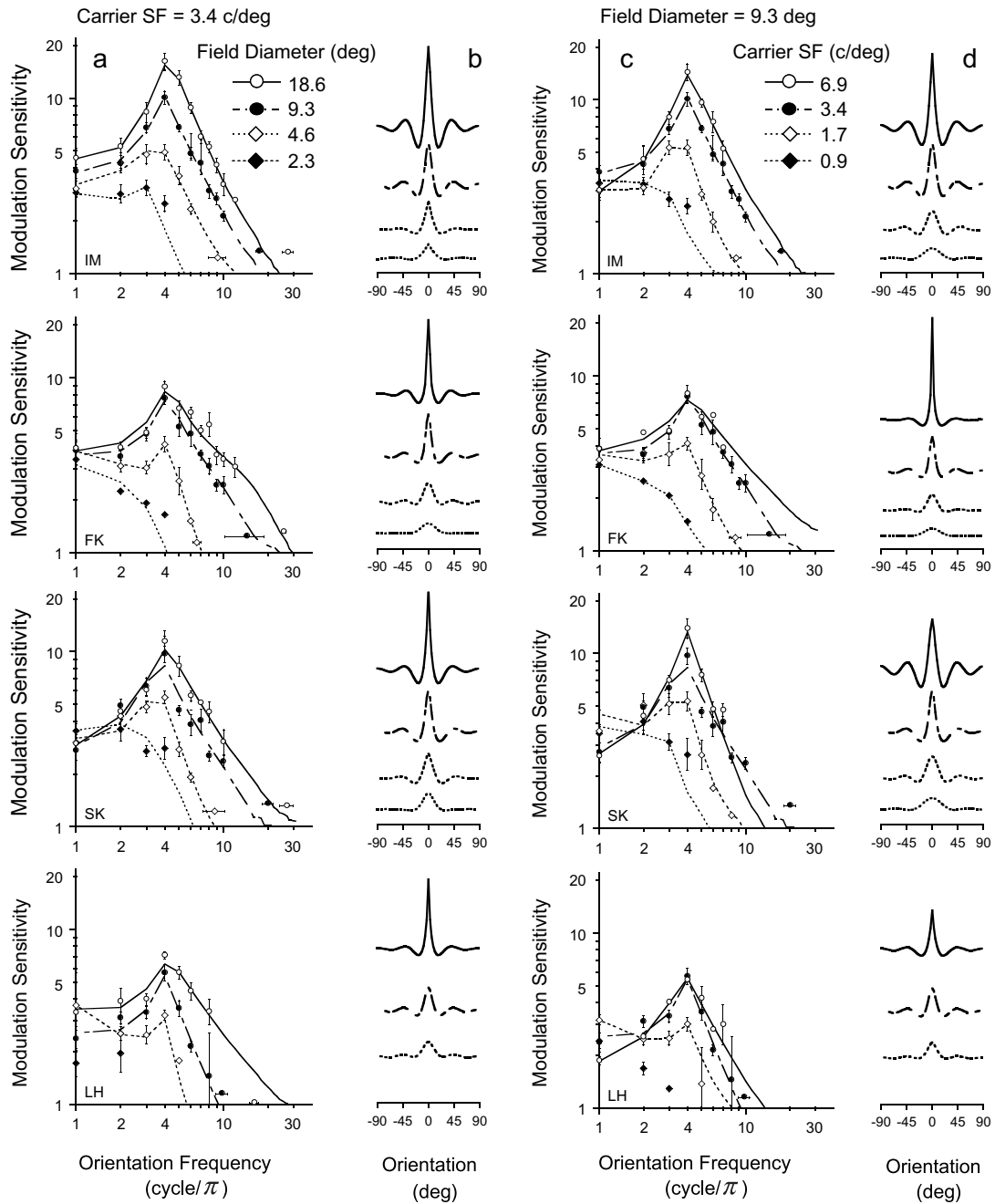


Fig. 3. (a, c) sensitivities for orientation-energy modulations as a function of orientation frequency in cycles/ π , for various stimulus sizes (a: carrier spatial frequency was constant at 3.4 cycles/deg), and for various carrier spatial frequencies (c: stimulus size was constant at 9.3 deg). Each panel shows the results for each observer. Symbols in (a) give stimulus diameter, and in (c) spatial frequency. Error bars represents ± 1 SD. Smooth curves are the sum-of-two-exponentials fitted to the data (see text). (b, d) Line spread functions in the orientation domain, calculated by inverse Fourier transform of the fitted sensitivity functions.

We obtained similar results when the centre spatial frequency of the noise was varied while keeping stimulus size constant in visual angle at 9.3 deg (Fig. 3c and d), suggesting that the cross-orientation antagonism depends upon field size *relative* to carrier wavelength (λ). This indicates that sensitivity to our energy-modulated stimuli is scale, or viewing-distant invariant.

In both Fig. 3b and d, the amplitude of the inhibitory lobes (and also secondary excitatory ones) begins close to zero when the relative stimulus size is small, and increases steadily as the relative stimulus size is increased. Increasing relative stimulus size also enhances overall sensitivity. Fig. 4 shows the amplitude of the excitatory (black) and inhibitory (gray) parts of the functions in

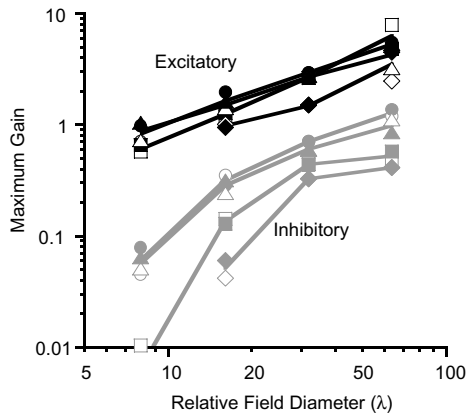


Fig. 4. Dependence of the excitatory and inhibitory lobe gains on relative stimulus size. The maximum excitatory (black) and inhibitory (gray) gains in the line spread function in Fig. 3b and d are plotted against stimulus diameter given in multiples of noise carrier wavelength λ . Open symbols are results for various stimulus sizes in degrees of visual angle (Fig. 3b), and closed symbols are results for various spatial frequencies (Fig. 3d). Lines are averages between the two. Different symbols represent different subjects.

Fig. 3b and d, plotted against relative stimulus size expressed in units of carrier wavelength (λ). The resulting functions obtained from Fig. 3b (varying size) and d (varying spatial frequency) overlap each other quite well, further suggesting scale invariance. The functions have slopes of $\cong 1$ on log–log axes up to and including a diameter of 64λ . The inhibitory parts, which are virtually absent at the smallest size of 8λ , rapidly increase with stimulus size up to 16λ , and then continue to increase steadily and in parallel with the central excitatory region.

4. Discussion

The present study investigated sensitivity for energy modulations of visual noise across orientation. The results can be summarized as follows. (1) The sensitivity function had a band-pass characteristic across orientation frequency, and this was modelled by a filter with a centre-surround antagonism across orientation, with inhibitory lobes at ± 15 – 20 deg. (2) For a given carrier wavelength λ , sensitivity increased with stimulus diameter with a slope of $\cong 1$ on log–log axes up to 64λ , and for a given stimulus diameter sensitivity decreased with λ with a similar slope, suggesting that sensitivity to orientation-energy-modulated stimuli is scale-invariant. (3) The cross-orientation antagonism was absent when the stimulus was small ($<16\lambda$).

Keeble et al. (1995) also examined the orientation characteristics of second-order processing using line-element textures, in which the probability of line segments having specific orientations was sinusoidally modulated across orientation. In contrast to the present

results, they found no evidence for cross-orientation antagonism; the sensitivity function was nearly low-pass against orientation frequency. Why the difference in results? One factor lies in the nature of the stimuli employed by Keeble et al. (1995). With their stimuli, the modulation depth of orientation energy rapidly decreased with modulation frequency because the line elements themselves had a considerable orientation bandwidth. The decline in orientation-energy with modulation frequency resulting from the spectral content of the stimuli may have counteracted the initial rise in perceptual sensitivity. We confirmed that when the sensitivity function in Keeble et al.'s study was divided by the Fourier transform of the line segment's orientation-tuning function, qualitatively similar results to ours was obtained.

4.1. Are the results about second-order vision?

The present study aimed to examine the orientation characteristics of second-order mechanisms. However, our energy-modulated stimulus differed in its first-order spectral content from the isotropic-noise stimulus against which it was discriminated, and hence one must consider whether the task could have been performed by subjects detecting a difference in a first-order, as opposed to second-order process. Two stimulus manipulations made this unlikely; first we randomised the contrast of each stimulus, second we randomised the phase of the energy modulation. Under these conditions it is difficult to see how the output of any first-order mechanism could have provided a reliable enough signal to do the task. Moreover, the results themselves implicate second-order rather than first-order process. First, the bandpass shape of the sensitivity function cannot be explained by the orientation-tuning of first-order filters (De Valois & De Valois, 1990; Ferster & Miller, 2000; Hubel & Wiesel, 1968), these are conventionally modelled as Gaussian, and if solely mediating the detection of the stimuli would predict the sensitivity function to be low-pass. Second, the scale invariant property of our stimuli is a prototypical signature of second-order rather than first-order processing (Kingdom & Keeble, 1999; Kingdom et al., 1995; Landy & Bergen, 1991; Sutter et al., 1995). Third, the increase in sensitivity with stimulus size with a slope of $\cong 1$ on log–log axes, up to 64λ cannot be simply ascribed to probability summation among relatively small detection mechanisms (but see later discussion). Instead it suggests a second-order process that operates over a wide spatial range, far beyond the size of the classical receptive field of first-order filters ($<2\lambda$). Finally, the lack of cross-orientation antagonism with small stimuli is difficult to understand in terms of the spatial properties of first-order filters. It rather suggests that inhibition is absent within small

regions of the centre of the second-order filter's receptive field, and that inhibition must originate from more distal regions.

4.2. Orientation opponent channels

Within the filter–rectify–filter framework, the cross-orientation antagonism revealed here suggests that second-order filters differentiate the outputs of orientation-selective first-order filters across orientation. One can plausibly term such functional mechanisms ‘orientation-opponent’ channels, analogous to the well-known ‘colour-opponent’ channels in colour vision that differentiate cones with different wavelength selectivities (Ingling, 1977; Jacobs & De Valois, 1965). Indeed, a computational scheme involving differentiation across orientation is reasonable in terms of the efficient coding of orientation and orientation-difference information in the natural image (Barlow, 1961). A recent statistical analysis of the orientation structure in natural images reveals co-occurrence of similar orientations among spatially local regions (Geisler, Perry, Super, & Gallogly, 2001). Similar opponent processes have been also proposed for motion (Allman, Miezin, & McGuinness, 1985) and depth perception (Neri, Parker, & Blakemore, 1999), implying a common strategy of visual information processing in the brain. Energy–frequency analysis could also be applied as an effective psychophysical tool for characterising the opponency along those dimensions.

The present analysis indicates that the putative orientation-opponent channel (1) has dominant opponency not between orthogonal orientations as has been suggested (Landy & Bergen, 1991), but between orientations 15–20 deg apart, (2) covers a wide spatial area, and (3) lacks opponency within a small central region. These features allow us to put forward a possible scheme in Fig. 5 for the receptive field organisation of the orientation-opponent channel. The channel is excited by the rectified first-order inputs of similar orientations in the central region of the receptive field, whereas in the surround region, the channel is excited by similar orientations to the centre, but inhibited by orientations at 15–20 deg.

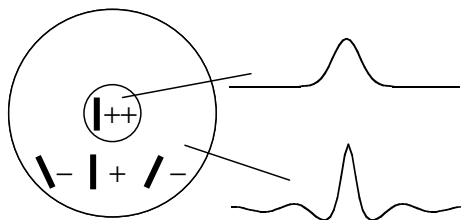


Fig. 5. Schematic diagram of the orientation-opponent channel. The channel is excited by a particular orientation in both the centre and surround of the receptive field, and inhibited by slightly different orientations, but only in the surround region.

The opponency between diagonal (15–20 deg) orientations is effective not only in detecting orientation-defined structure in textures, but also in sharpening the tuning for orientation itself. The putative orientation-opponent channel, with its spatially wide operation, may underlie the high accuracy for global orientation perception (Dakin, 2001; Kingdom et al., 1995; Orban, Vandebussche, & Vogels, 1984), since the opponent process amplifies the difference in the output of first-order filters tuned to two orientations before they are compared. In addition, opponency between diagonal orientations predicts the classical tilt illusion, where the apparent orientation of a stimulus is shifted away from a stimulus having slightly different orientations because the peak in the response distribution, which is often regarded as corresponding to the perceived orientation, to the stimulus is shifted as a result of inhibition from diagonal orientations (Blakemore, Carpenter, & Georgeson, 1970; Braddick, Campbell, & Atkinson, 1978).

The receptive-field in Fig. 5 looks somewhat complex in terms of orientation selectivity, and may be the computational equivalent of multiple classes of sub-channels having simpler receptive-field structures, as proposed for colour-opponent channels. Moreover, our data does not necessarily indicate that the orientation-opponent channel has a circular receptive field, as shown. An impression of ‘streaks’ in our stimuli (Fig. 2) implies that it might have an elongated receptive field, pooling the signals from collinearly aligned orientation-selective first-order inputs along its axis (Dakin & Mareschal, 2000; Field, Hayes, & Hess, 1993; Kapadia, Westheimer, & Gilbert, 2000; Polat & Sagi, 1993). It should be noted, however, that simple collinear pooling *without orientation opponency* predicts highest sensitivity for energy modulations at 1 cycle/ π in which the collinear structure is physically the most evident, suggesting that orientation opponency is essentially required to account for our results.

It is important to note that the orientation opponency revealed here does not necessarily indicate a general property of second-order visual processing. It has been suggested that distinct classes of second-order mechanism are involved in the detection of spatial modulations in different stimulus attributes (Cavanagh, Arguin, & Treisman, 1990), or that different spatial modulations are subserved by a single class of second-order mechanism, but one with different carrier tunings (Kingdom, Prins, & Hayes, 2003), and it is entirely possible that orientation-opponency is restricted to a subset of them. Moreover, there is some evidence for a broad division of second-order mechanisms into edge-based and region-based (Gurnsey & Laundry, 1992; Wolfson & Landy, 1998), with edge-based mechanisms being implicated in some types of texture segmentation, and region-based mechanisms being implicated primarily in tasks that

require subjects to discriminate two uniform textures separated in time, as here. The structure of the model filter in Fig. 5 nevertheless raises the possibility that it may also be involved in texture segmentation, and indeed we have recently confirmed the operation of orientation opponency in spatially modulated texture detection.

4.3. Neural basis of orientation opponency

What is the neural substrate of such narrowly tuned orientation opponency? One candidate is the cross-orientation inhibition believed to play a critical role in the contrast-gain control and orientation sharpening of individual neurons in V1 (Bonds, 1989; Burr & Morrone, 1987; Carandini, Heeger, & Movshon, 1997; DeAngelis, Robson, Ohzawa, & Freeman, 1992; Ferster & Miller, 2000; Heeger, 1992; Morrone, Burr, & Maffei, 1982; Ringach, 1998; Ringach, Hawken, & Shapley, 1997; Sillito, 1975). Contrast gain control, in principle, is able to account for the present psychophysical data. Fig. 6 shows the sensitivity functions simulated with a simplified version of a contrast gain control model. The model assumes that the excitatory input to the mechanism is from one range (σ_e) of orientations, and that this is divided by inhibitory inputs from another range (σ_i) of orientations (see Appendix A). If both inputs have broad orientation tunings (e.g., $\sigma_e = 15$ deg and $\sigma_i = 45$ deg), as suggested by physiological (Bonds, 1989; Burr & Morrone, 1987; Carandini et al., 1997; De Valois & De Valois, 1990; Heeger, 1992; Morrone et al., 1982) and psychophysical (Foley, 1994; Ross & Speed, 1991) studies, the model incorrectly predicts a low-pass sensi-

tivity function (open circles in Fig. 6). If the orientation tunings of the both inputs are assumed to be very sharp however (e.g., $\sigma_e = 5$ deg and $\sigma_i = 15$ deg: filled circles in Fig. 6), a quantitatively comparable sensitivity function is obtained. Thus contrast gain control can explain the results of the present study if one assumes that the visual system has mechanisms with very sharp orientation tunings. There is evidence for small populations of neurons with such sharp orientation tunings (5–6 deg; De Valois & De Valois, 1990). On the other hand, it has been argued that the cross-orientation inhibition implicated in contrast gain control is mostly restricted to within the classical receptive field (DeAngelis et al., 1992), and that the orientation bandwidth of cortical neurons changes with their spatial frequency tunings (De Valois & De Valois, 1990). These features seem inconsistent with the large area summation, scale invariance, and the absence at small stimuli, of the orientation opponency found here, although one can still ascribe them as a characteristics of some higher-order processes that integrate the gain-controlled outputs of local units.

Another candidate neural substrate is the response suppression observed by stimuli outside of the classical receptive field, which is considered to play an important role in texture analysis (Blakemore & Tobin, 1972; Maffei & Fiorentini, 1976; Zipser, Lamme, & Schiller, 1996). Recent neurophysiological studies suggest that this surround suppression, like contrast gain control, can be characterised as divisive inhibition (Cavanaugh, Bair, & Movshon, 2002), although it has been pointed out that surround suppression is mediated by a different form of gain change from that of contrast-gain control (Sengpiel, Baddeley, Freeman, Harrad, & Blakemore, 1998). However the orientation tuning of surround suppression appears to be narrowly tuned to the same orientation as the target neuron (Cavanaugh et al., 2002), which is not consistent with the model in Fig. 5 that encapsulates our data. As noted above, however, there is also evidence for other types of surround modulation, for example facilitatory interactions between collinearly aligned neurons. Therefore a combination of different types of surround modulation, together with local contrast-gain control, may turn out to provide the best account of the orientation opponency revealed here.

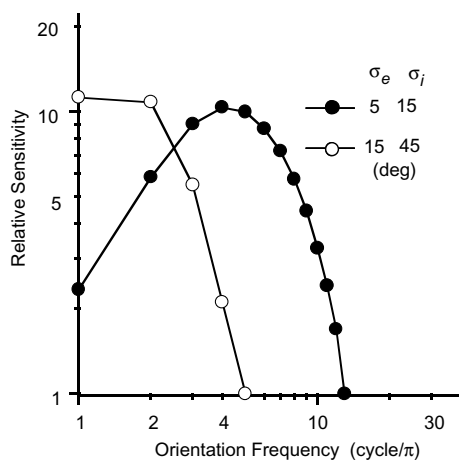


Fig. 6. Sensitivity to cross-orientation energy modulations predicted by a divisive contrast gain control model. Open circles represent the results of a simulation in which the mechanism's excitatory and inhibitory inputs have orientation bandwidths of 15 and 45 deg, respectively. Filled circles represent the results when the excitatory and inhibitory orientation bandwidths are 5 and 15 deg, respectively. See text for details.

Acknowledgements

The authors thank Stephane Rainville for pointing out a potential artefact in our stimuli, Curtis Baker for comments on the early version of the draft, and two anonymous reviewers and the editor for thoughtful suggestions. Supported by a JSPS research fellowship (Tohoku University) given to IM, and NSERC (Canada) grant ref.: OGP 01217130 given to FK.

Appendix A

We employed a simplified model of contrast gain control in which the computations were carried out entirely in the orientation domain, i.e. not in the conventional, space domain. The model cortical mechanism consisted of a Gaussian excitatory function of orientation $E(\theta)$ with a standard deviation of σ_e , and a Gaussian inhibitory function of orientation $I(\theta)$ with standard deviation of σ_i . These two functions were separately convolved with the sinusoidal function that described the orientation-energy modulation in the stimulus, and then subject to a Naka–Rushton function resulting in a response $R(\theta)$ given by:

$$R(\theta) = A \frac{E(\theta)^p}{Z + I(\theta)^q}, \quad (\text{A.1})$$

where A , p , q , and Z are parameters given below. Thresholds for energy modulations at various orientation frequencies were estimated by calculating the minimum modulation depth that gave a unit difference (1.0) with the response to the unmodulated stimulus. Sensitivity was given as an inverse of the threshold. In the results of the simulation shown in Fig. 6, A , p , q , and Z were set to 50.0, 2.2, 2.0, and 0.1, and σ_e and σ_i were 5 and 15 deg (filled circles), or 15 and 45 deg (open circles).

References

- Allman, J., Miezin, F., & McGuinness, E. (1985). Stimulus specific response from beyond the classical receptive field: neurophysiological mechanisms for local-global comparisons in visual neurons. *Annual Review of Neuroscience*, *8*, 407–430.
- Arsenault, A. S., Wilkinson, F., & Kingdom, F. A. (1999). Modulation frequency and orientation tuning of second-order texture mechanisms. *Journal of the Optical Society of America A*, *16*, 427–435.
- Barlow, H. B. (1961). Possible principles underlying the transformation of sensory messages. In W. A. Rosenblith (Ed.), *Sensory communication*. Cambridge: MIT Press.
- Barlow, H. B. (1982). What causes trichromacy? A theoretical analysis using comb-filtered spectra. *Vision Research*, *22*, 635–643.
- Blakemore, C., Carpenter, R. H., & Georgeson, M. A. (1970). Lateral inhibition between orientation detectors in the human visual system. *Nature*, *228*, 37–39.
- Blakemore, C., & Tobin, E. A. (1972). Lateral inhibition between orientation detectors in the cat visual cortex. *Experimental Brain Research*, *15*, 439–440.
- Bonds, A. B. (1989). Role of inhibition in the specification of orientation selectivity of cells in the cat striate cortex. *Visual Neuroscience*, *2*, 41–55.
- Braddick, O., Campbell, F. W., & Atkinson, J. (1978). Channels in vision: basic aspects. In R. Held, H. W. Leibowitz, & H. L. Teuber (Eds.), *Handbook of sensory physiology* (Vol. VIII). Berlin: Springer-Verlag.
- Burr, D. C., & Morrone, M. C. (1987). Inhibitory interactions in the human visual system revealed in pattern-evoked potentials. *Journal of Physiology*, *389*, 1–21.
- Carandini, M., Heeger, D. J., & Movshon, J. A. (1997). Linearity and normalization in simple cells of the macaque primary visual cortex. *Journal of Neuroscience*, *17*, 8621–8644.
- Cavanagh, P., Arguin, M., & Treisman, A. (1990). Effects of surface medium on visual search for orientation and size features. *Journal of Experimental Psychology: Human Perception, Performance*, *16*, 479–491.
- Cavanaugh, J. R., Bair, W., & Movshon, J. A. (2002). Selectivity and spatial distribution of signals from the receptive field surround in macaque V1 neurons. *Journal of Neurophysiology*, *88*, 2547–2556.
- Chubb, C., & Sperling, G. (1988). Drift-balanced random stimuli: a general basis for studying non-Fourier motion perception. *Journal of the Optical Society of America A*, *5*, 1986–2007.
- Dakin, S. C. (2001). Information limit on the spatial integration of local orientation signals. *Journal of the Optical Society of America A*, *18*, 1016–1026.
- Dakin, S. C., & Mareschal, I. (2000). Sensitivity to contrast modulation depends on carrier spatial frequency and orientation. *Vision Research*, *40*, 311–329.
- De Valois, R. L., & De Valois, K. K. (1990). *Spatial vision*. New York: Oxford University Press.
- DeAngelis, G. C., Robson, J. G., Ohzawa, I., & Freeman, R. D. (1992). Organization of suppression in receptive fields of neurons in cat visual cortex. *Journal of Neurophysiology*, *68*, 144–163.
- Ferster, D., & Miller, K. D. (2000). Neural mechanisms of orientation selectivity in the visual cortex. *Annual Review of Neuroscience*, *23*, 441–471.
- Field, D. J., Hayes, A., & Hess, R. F. (1993). Contour integration by the human visual system: evidence for a local “association field”. *Vision Research*, *33*, 173–193.
- Foley, J. M. (1994). Human luminance pattern-vision mechanisms: masking experiments require a new model. *Journal of the Optical Society of America A*, *11*, 1710–1719.
- Geisler, W. S., Perry, J. S., Super, B. J., & Gallogly, D. P. (2001). Edge co-occurrence in natural images predicts contour grouping performance. *Vision Research*, *41*, 711–724.
- Goda, N., & Fujii, M. (2001). Sensitivity to modulation of color distribution in multicolored textures. *Vision Research*, *41*, 2475–2485.
- Graham, N. (1994). Complex channels, early local non-linearities, and normalization in texture segregation. In M. S. Landy, & J. A. Movshon (Eds.), *Computational models of visual processing*. Cambridge: MIT Press.
- Gray, R., & Regan, D. (1998). Spatial frequency discrimination and detection characteristics for gratings defined by orientation texture. *Vision Research*, *38*, 2601–2617.
- Gurnsey, R., & Laundry, D. S. (1992). Texture discrimination with and without abrupt texture gradients. *Canadian Journal of Psychology*, *46*, 306–332.
- Heeger, D. J. (1992). Normalization of cell responses in cat striate cortex. *Visual Neuroscience*, *9*, 181–197.
- Hubel, D. H., & Wiesel, T. N. (1968). Receptive fields and functional architecture of monkey striate cortex. *Journal of Physiology*, *195*, 215–243.
- Ingling, C. R., Jr. (1977). The spectral sensitivity of the opponent-color channels. *Vision Research*, *17*, 1083–1089.
- Jacobs, G. H., & De Valois, R. L. (1965). Chromatic opponent cells in squirrel monkey lateral geniculate nucleus. *Nature*, *206*, 487–489.
- Kapadia, M. K., Westheimer, G., & Gilbert, C. D. (2000). Spatial distribution of contextual interactions in primary visual cortex and in visual perception. *Journal of Neurophysiology*, *84*, 2048–2062.
- Keeble, D. R., Kingdom, F. A., Moulden, B., & Morgan, M. J. (1995). Detection of orientationally multimodal textures. *Vision Research*, *35*, 1991–2005.
- Kingdom, F. A., & Keeble, D. R. (1996). A linear systems approach to the detection of both abrupt and smooth spatial variations in orientation-defined textures. *Vision Research*, *36*, 409–420.
- Kingdom, F. A. A., & Keeble, D. R. T. (1999). On the mechanism for scale invariance in orientation-defined textures. *Vision Research*, *39*, 1477–1489.

- Kingdom, F. A., Keeble, D., & Moulden, B. (1995). Sensitivity to orientation modulation in micropattern-based textures. *Vision Research*, 35, 79–91.
- Kingdom, F. A. A., Prins, N., & Hayes, A. (2003). Mechanism independence for texture-modulation detection is consistent with a filter–rectify–filter mechanism. *Visual Neuroscience*, 20, 65–76.
- Landy, M. S., & Bergen, J. R. (1991). Texture segregation and orientation gradient. *Vision Research*, 31, 679–691.
- Landy, M. S., & Oruc, I. (2002). Properties of second-order spatial frequency channels. *Vision Research*, 42, 2311–2329.
- Maffei, L., & Fiorentini, A. (1976). The unresponsive regions of visual cortical receptive fields. *Vision Research*, 16, 1131–1139.
- Malik, J., & Perona, P. (1990). Preattentive texture discrimination with early vision mechanisms. *Journal of the Optical Society of America A*, 7, 923–932.
- Morrone, M. C., Burr, D. C., & Maffei, L. (1982). Functional implications of cross-orientation inhibition of cortical visual cells. I. Neurophysiological evidence. *Proceedings of the Royal Society of London B*, 216, 335–354.
- Neri, P., Parker, A. J., & Blakemore, C. (1999). Probing the human stereoscopic system with reverse correlation. *Nature*, 401, 695–698.
- Orban, G. A., Vandenbussche, E., & Vogels, R. (1984). Human orientation discrimination tested with long stimuli. *Vision Research*, 24, 121–128.
- Polat, R., & Sagi, D. (1993). Lateral interactions between spatial channels: suppression and facilitation revealed by lateral masking experiments. *Vision Research*, 33, 993–999.
- Ringach, D. L. (1998). Tuning of orientation detectors in human vision. *Vision Research*, 7, 963–972.
- Ringach, D. L., Hawken, M. J., & Shapley, R. (1997). Dynamics of orientation tuning in macaque primary visual cortex. *Nature*, 387, 281–284.
- Ross, J., & Speed, H. D. (1991). Contrast adaptation and contrast masking in human vision. *Philosophical Transactions of the Royal Society of London B*, 246, 61–69.
- Sengpiel, F., Baddeley, R. J., Freeman, T. C. B., Harrad, R., & Blakemore, C. (1998). Characteristics of surround inhibition. *Vision Research*, 38, 2067–2080.
- Sillito, A. M. (1975). The contribution of inhibitory mechanisms to the receptive field properties of neurones in the striate cortex of the cat. *Journal of Physiology*, 250, 305–329.
- Sutter, A., Sperling, G., & Chubb, C. (1995). Measuring the spatial frequency selectivity of second-order texture mechanisms. *Vision Research*, 35, 915–924.
- Tyler, C. W. (1974). Depth perception in disparity gratings. *Nature*, 251, 140–142.
- Watson, A. B., & Eckert, M. P. (1994). Motion-contrast sensitivity: visibility of motion gradients of various spatial frequencies. *Journal of the Optical Society of America A*, 11, 496–505.
- Wilson, H. R. (1993). Nonlinear processes in visual pattern discrimination. *Proceedings of the National Academy of Sciences of the United States of America*, 90, 9785–9790.
- Wolfson, S. S., & Landy, M. S. (1998). Examining edge- and region-based texture analysis mechanisms. *Vision Research*, 38, 439–446.
- Zipser, K., Lamme, V. A., & Schiller, P. H. (1996). Contextual modulation in primary visual cortex. *Journal of Neuroscience*, 16, 7376–7389.